

STRAIN AGING PHENOMENA IN SILVER CHLORIDE

著者	FUKAI Akira, SLIFKIN Lawrence M.
journal or publication title	鹿児島大学理学部紀要. 数学・物理学・化学
volume	3
page range	17-32
別言語のタイトル	塩化銀における時効硬化現象
URL	http://hdl.handle.net/10232/00010019

STRAIN AGING PHENOMENA IN SILVER CHLORIDE

By

Akira FUKAI and Lawrence M. SLIFKIN*

(Received September 30, 1970)

Abstract

Strain aging phenomena have been observed at room temperature and are discussed in the light of the current dislocation pinning model. It has become quite evident from the analysis, in conformity to the work of Kabler, Miller and Slifkin, that the fresh dislocations introduced into the sample on handling are gradually pinned by diffusing impurity ions. The rate of pinning by diffusing defects is found to be larger than that predicted by Cottrell. It is suspected that this discrepancy is due to the electrostatic attractive interaction between impurity ions and the charge on the dislocations. During the aging process, the distance between minor pins tends to a saturation value. This gives 0.22 eV as the binding energy between dislocations and pinning defects.

Introduction

Kabler, Miller and Slifkin¹⁾ have extensively studied the strain aging phenomena in AgCl near the room temperatures. The authors identified the cause of strain aging to be the divalent impurity atoms that diffuse to the fresh dislocation during an incubation time and then act as pinning agents. This type of recovery phenomena has also been reported by Russian workers²⁾³⁾ who measured the internal friction of thin wires of polycrystalline silver chloride at low frequencies as a function of time after deformation.

The present paper will discuss the kinetics of these phenomena in the light of internal friction work.

The dislocation pinning model developed by Granato and Lücke consists of an edge dislocation pinned by two types of pinning agents, minor pins and major pins. The former may be solute atoms (impurity atoms), the latter, on the other hand, may be nodes of network. Minor pins interact with dislocations more weakly than major pins, so that only a small stress is necessary to unpin the dislocations from them. The average distances between minor pins and major pins are denoted L_c and L_N , respectively. If the temperature is high enough for diffusion of solute atoms to take place, then the concentration on the dislocation, c , can attain an equilibrium value according to

$$c = a/L_c = c_0 e^{Q/kT}, \quad (1)$$

where Q is Cottrell's interaction energy between a dislocation and impurity atom; a , the lattice parameter; c_0 , bulk concentration; kT , the conventional meaning. The average free

* Department of Physics, University of North Carolina at Chapel Hill, Chapel Hill, N.C., U.S.A.
27515

length of dislocation is given by

$$L^{-1} = L_c^{-1} + L_N^{-1}. \quad (2)$$

With this model in mind, they have calculated the damping due to the motion of a dislocation of particular length of L by solving a differential equation similar to that for a vibrating string in a viscous media. There are two types of losses which result: (1) dynamic loss, (2) hysteresis loss. Dynamic loss corresponds to cyclic motion with a small amplitude and is found to have a maximum at certain frequency that usually falls in the megacycle range. Since this process is of the resonance type, frequency dependence and amplitude dependence result. For frequencies much less than the resonance frequency, the damping, δ_I , i.e. amplitude-independent decrement, can be expressed as

$$\delta_I = \frac{\Omega AL^4 B \omega t_1}{\pi^3 C} \quad (3)$$

Here Ω is an orientation factor taking into account the fact that the resolved shear stress on the slip plane is less than the applied longitudinal stress; A , the dislocation density; B , the damping constant of a moving dislocation; ω , the angular frequency; C , the tension of a dislocation line; t_1 , factors which depend on the distribution of loop lengths assumed. Hysteresis loss is caused by the breakaway of dislocation from the minor pinning point at the critical stress. Upon increasing the stress, the loops tend to bow out until the stress level reaches σ_c . At this critical stress, the strain greatly increases with little or no increase in applied stress. Beyond σ_c , the loop with length L_N bows out further. If σ is decreased, the strain will not take the same values as those for increasing stress, thus resulting in hysteresis. By calculating the damping loss due to this hysteresis, with appropriate assumptions of the distribution of loop lengths, Granato and Lücke calculated this as

$$\delta_H = \frac{\Omega AL_N^3}{\pi^3 L_c} \frac{K \eta a}{L_c \epsilon} e^{-\frac{K \eta a}{L_c \epsilon_0}}. \quad L_N \gg L_c \gg a \quad (4)$$

Here K is an orientation-dependent factor connected with the stress necessary for breakaway. η is Cottrell's misfit parameter. It follows from this formula that a plot of $\ln(\delta_H \cdot \epsilon)$ vs. $1/\epsilon$ should be a straight line, if this model is applicable to the solid in question. The slope and intersection at $1/\epsilon=0$, would, then, be proportional to $1/L_c$ (that is, to the concentration of impurities on the dislocation) and to the dislocation density, respectively. It has been found that this relation, hereafter called the Granato-Lücke plot, is surprisingly successful in many cases. The dependence of δ_H on several parameters, such as impurity concentration, dislocation density, temperature, time, etc., has given some credence on this pinning model.

Experimental Procedures and Specimens

Experimental procedures in the present work is essentially the same as mentioned in

the previous publication.⁴⁾ Marx method using the composite quartz resonator was adopted at the frequency of 35kHz.

Specimens used in this work are all of normal purity, the conductivity ranging from 3×10^{-8} to $8 \times 10^{-8} \Omega^{-1} \text{cm}^{-1}$. Annealings of specimens were done at approximately 430°C for a day before the measurements to remove mechanical strain induced in the crystals.

Results

The decrement in the strain-independent region has been observed to decrease rapidly

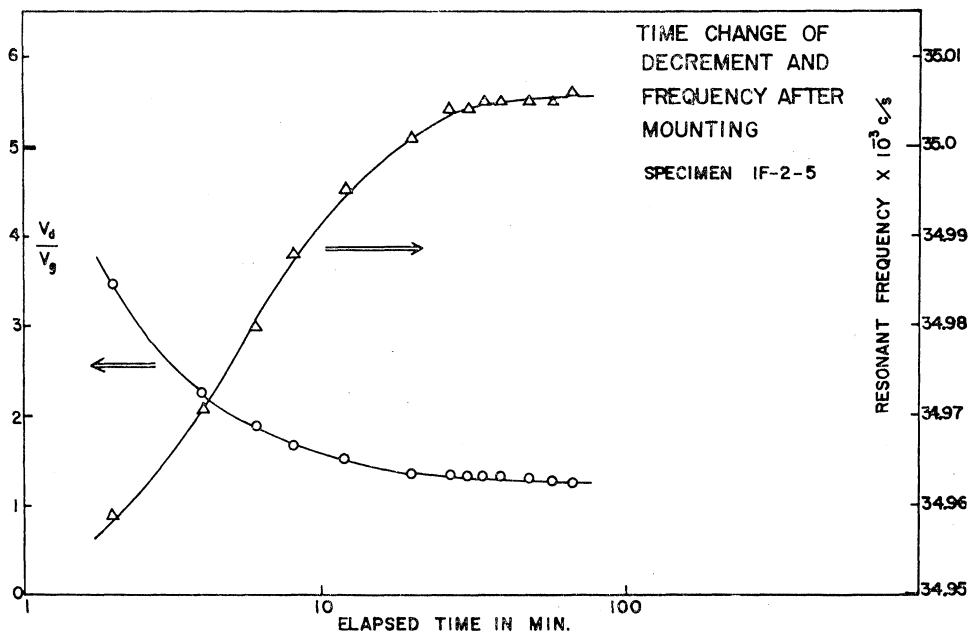


Fig. 1

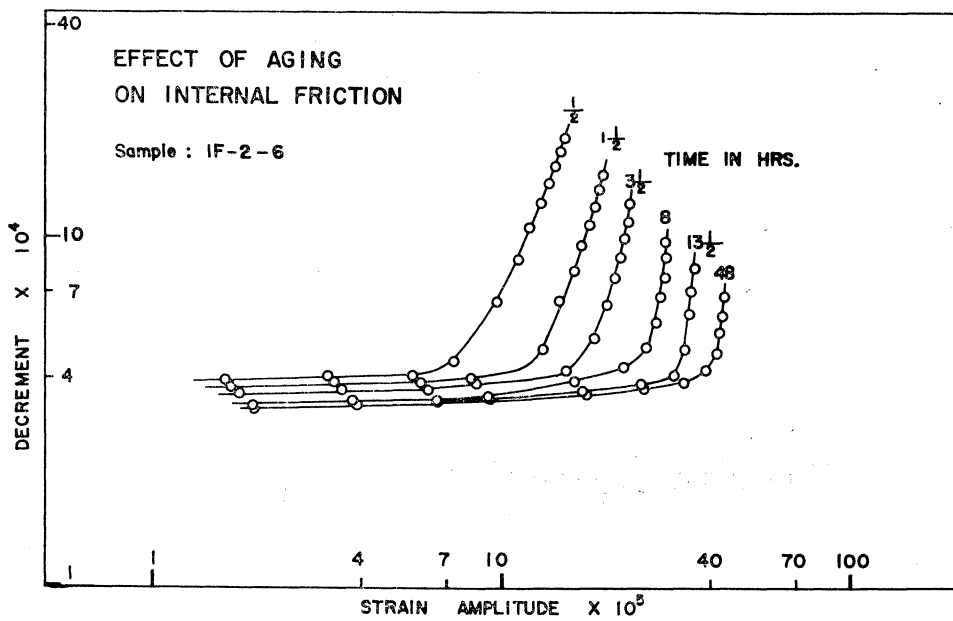


Fig. 2

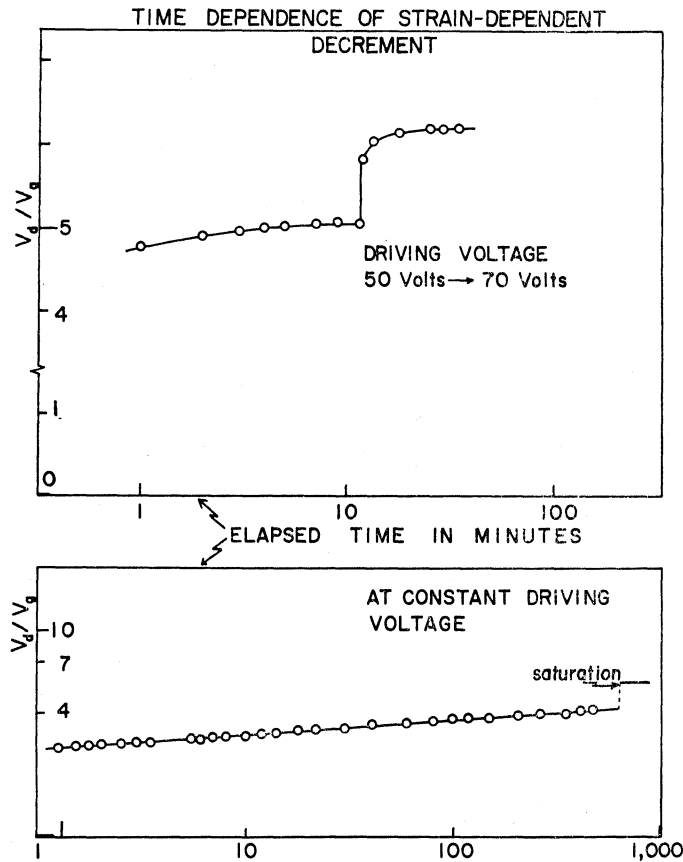


Fig. 3

during the first twenty minutes after mounting, accompanied by an increase in the resonant frequency. This decrease in decrement continues for a day or two with decreasing rate as shown in Figure 1, along with the associated increase in resonant frequency. For the first twenty minutes in most cases, it was impossible to measure the strain-dependent decrement because of its rapid change. The quantity V_d/V_g , the ratio of input voltage to output voltage in the quartz resonator assembly, is proportional to the decrement for the total system, so the decrement of specimen must be changing more rapidly than shown in the figure, since the total decrement is the mass-weighted mean of that of the sample and background, the mass ratio being usually of the order of 3. The rate of change with time was not unique: sometimes an appreciable decrease in decrement was observed over two hours. The decrement vs. strain amplitude curves were measured 20 to 30 minutes after the mounting when the rate of change in decrement had become relatively slow. A typical example is shown in Fig. 2. The shift of breakaway stress to higher value is clearly shown. The shift of the breakaway point was found to continue for as long as 72 hours in some cases, although the decrease of strain-independent decrement with time was not consistent; small variations were observed as a function of time. The saturated value of breakaway stress, i.e. the maximum strain amplitude obtained in the time sequence, was not unique even for a particular sample. For example, sample IF-2-6 had a breakaway

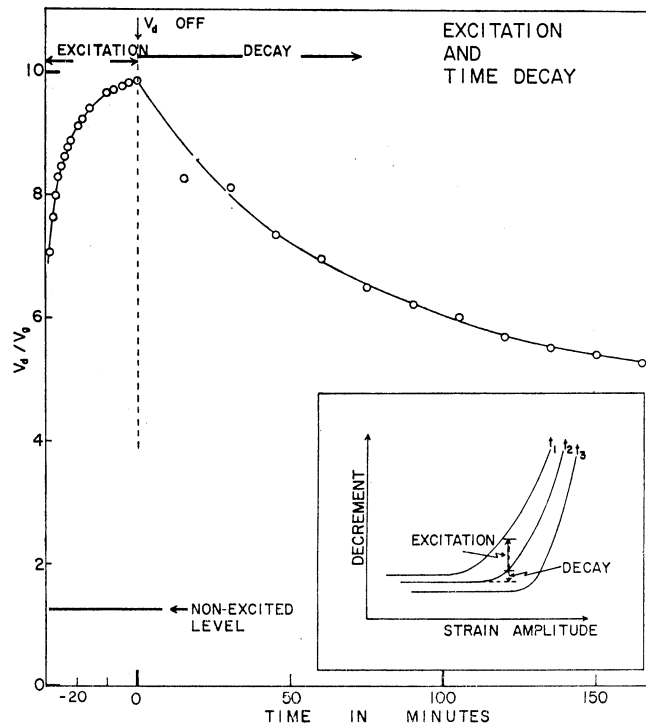


Fig. 4

stress in the range of 2×10^{-4} to 4×10^{-4} . It is worth while to mention that the time for the hysteresis of strain-dependent region to disappear varies from 1/2 hour in the early period to 3 hours later on. It must also be mentioned that each measurement in the strain amplitude-dependent region of the decrement vs. strain amplitude curve was taken 1 minute after the new driving voltage was applied.

Fig. 3 shows the time dependence of the strain-dependent decrement. The upper half of the figure shows how the decrement responded to a sudden increase of driving voltage; it always required a finite time to reach the saturation value. The strain amplitude-dependent decrement in the final stage of the time sequence was found to take an extremely long time to reach the saturation value after applying the driving voltage (see lower half of Figure 3). The stress in the crystal is actually decreasing as the decrement increases because of the constant driving voltage in this measurement; the ratio of the final stress to the original value in this measurement is about 1/2. Thus it is quite evident from this result that the mechanical state of crystal does not show an instant response, but gradually changes with time into a more stable state corresponding to the new stress. This time-dependence was observed only in the strain-dependent region.

Next, a series of experiments was performed to study the rate of decay from the excited state (i.e. the state reached after prolonged oscillatory stress) to the state in equilibrium with either no stress or a stress in the strain-independent region. Fig. 4 shows the result of such an experiment. The decay of decrement has been recorded at the same strain amplitude as used for excitation (in this particular case, driving voltage, proportional

to the strain amplitude, was 10 volts.). The quantity plotted on the vertical axis is V_d/V_g which is proportional to the total decrement. It is easily seen that for the discussion of the rate of change of the decrement of the specimen, one only needs to know V_d/V_g . The insert in this figure shows schematically how this time change in total decrement is related to the aging experiment. The measurement of the decay process must be done such that each measurement does not appreciably disturb the system. Since applying the driving voltage necessary for the purpose of spot measurement does actually increase the decrement, the time duration of the measurements must be made as short as possible. Ten seconds was adopted for the measuring time which was the minimum time possible with the present experimental apparatus. The time interval between successive measurements was 15 minutes. If the decrease of decrement shown in Fig. 4 is plotted P against time on a log-log scale, then Fig. 5 results. Here P is defined as

$$P = \ln \frac{\delta - \delta_0}{\delta_1 - \delta_0}, \quad (5)$$

where δ_0 is the decrement at the start of excitation, δ_1 is the decrement at the end of excitation and δ is the measured decrement during the decay process. The meaning of the quantity P , and the slope of the straight line in the diagram above will be seen in the following section. Within the experimental error these points seem to fall on a straight line with a slope of 0.71. It has been found in the course of this experiment that the progress of decay is influenced by how the spot measurement is done. Some results are shown in

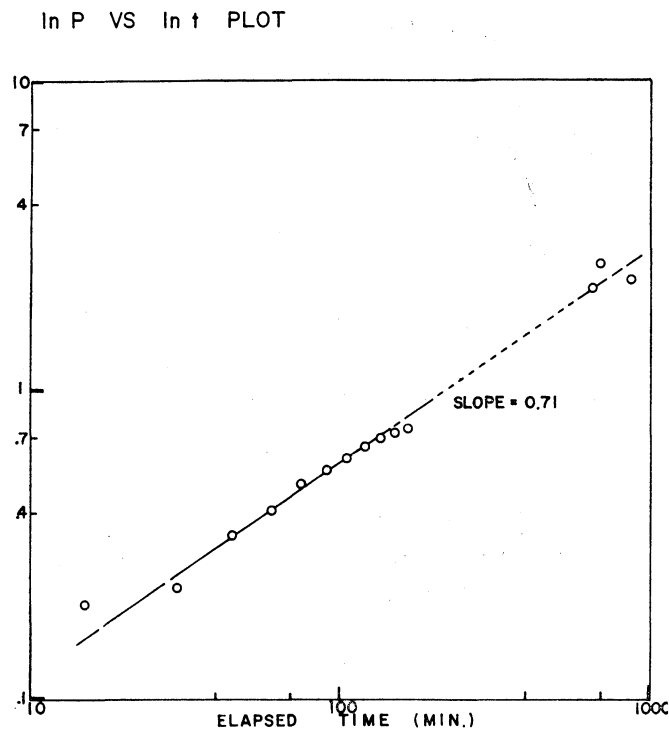


Fig. 5

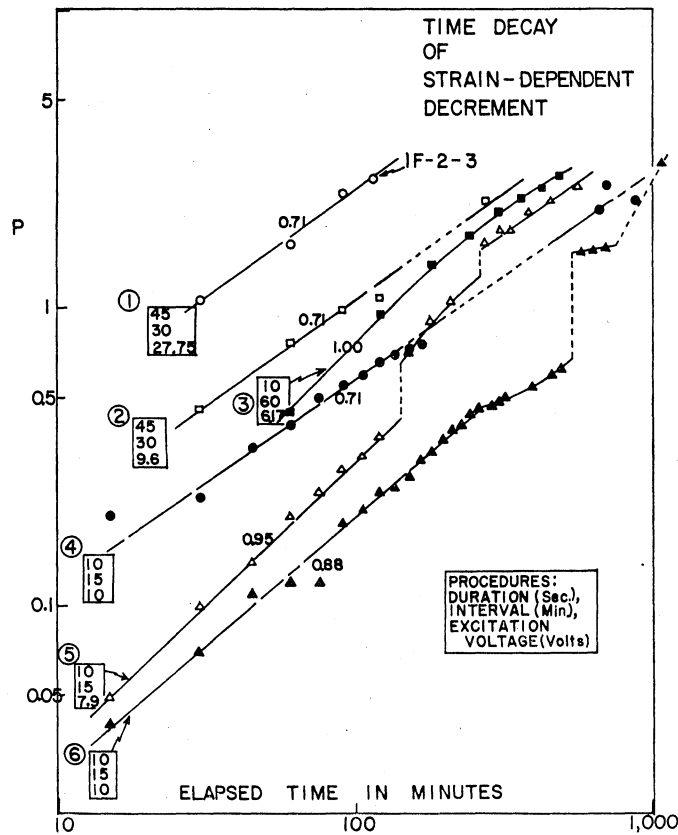


Fig. 6

Fig. 6, including the data in Fig. 5. Curves, 2, 3, 4, 5 and 6 are measured in the sample IF-2-6 while curve 1 is for IF-2-3. Noticeable are the following: (1) the initial portions seem to be linear and less influenced by the measurements themselves; the slope range 0.71 to 1.00 with the average close to 0.83; (2) long interval between measurements and extended times of spot measurement seem to give larger P , or faster decay; (3) if P in the initial stages is low, then a sudden increase occurs when the time interval between measurement is increased during the run, the P values in the final stages seem to tend to almost the same values.

Discussion

(a) Analysis of Decrement vs. Strain Amplitude Curves

In analyzing the time change in decrements after mounting, shown in Fig. 2, a Granato-Lücke plot has been constructed for each decrement vs. strain amplitude curve. The results, in Fig. 7, show that each series of measured points falls quite well on the predicted straight line, within the experimental error. Following the usual procedure, as mentioned in Introduction, we can obtain L_e and L_N from the slope of each straight line and the intersection with the vertical axis ($\epsilon^{-1}=0$). It must be admitted that, in comparison with earlier times, the slopes for later times cause considerably more error in obtaining $\delta \cdot \epsilon$ at $\epsilon^{-1}=0$.

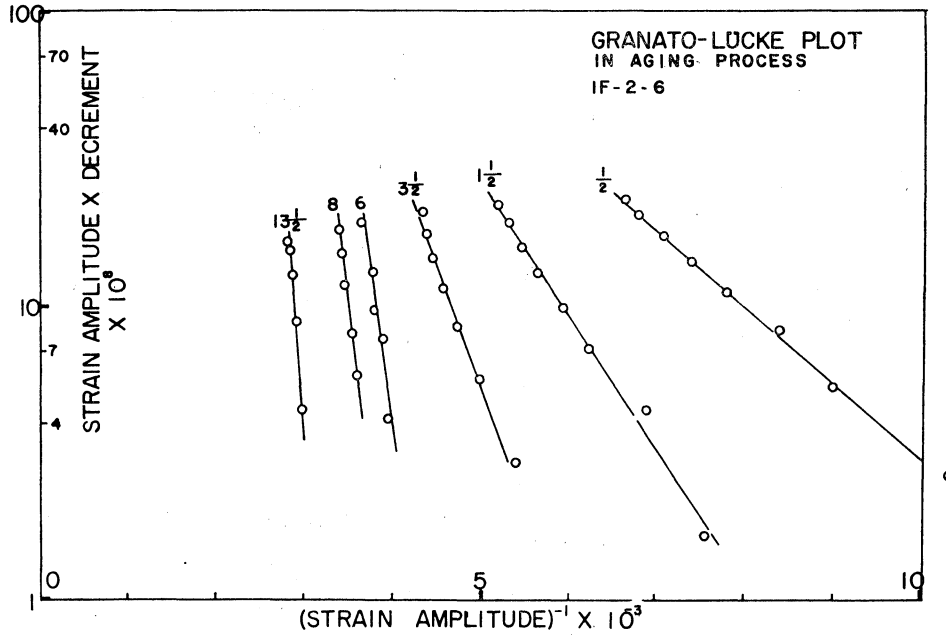


Fig. 7

In order to obtain L_c and L_N numerically, we must assume values for several of the parameters in Equation (4). For the calculation of L_c , the orientation-dependent factor K and Cottrell misfit parameter η must be known. η has been taken equal to 0.1, the same value employed by Granato and Lücke⁵). K is given as

$$K = \frac{32}{\pi^2 p^2} \frac{G}{RE} \quad (6)$$

where G is the shear modulus, R is the resolved shear stress factor and p is a constant with a value of about 2 or 3. With $G=1.1 \times 10^{11}$ dyne/cm², $E=2.5 \times 10^{11}$ dyne/cm² (mean of three major crystallographic orientations), $p=3$, $R=0.5$, we get $K=0.31$. Alternatively, if we choose the values $E=2 \times 10^{11}$ dyne/cm² and $p=2$, $K=0.89$ is obtained. By using $K=0.31$ and $\eta=0.1$, the mean distance L_c between minor pinning points at the earliest time becomes 50 atomic distances. L_c at later stages, when it becomes saturated, is found to be 2 atomic distances. If K is taken as 0.89, L_c becomes accordingly three times as large as the ones just quoted. The ratio of L_c with time for $K=0.31$, along with other quantities that will be shortly discussed, is shown in Fig. 8. The error of determining the slope of G-L plot at the saturated state may allow L_c to be in the range between 2 and 3 atomic distances for $K=0.31$, 6 and 9 atomic distances for $K=0.89$.

In what follows, L_c will be taken as 6 atomic distances. Simply by taking the inverse of L_c , the concentration of pinning defects c_{disl} on the dislocations is obtained. This necessarily saturates as L_c becomes constant. This result suggests that the dislocation initially with few pinning points gradually collects point defects. If these pinning points are in thermal equilibrium with surrounding, we can calculate the binding energy U between

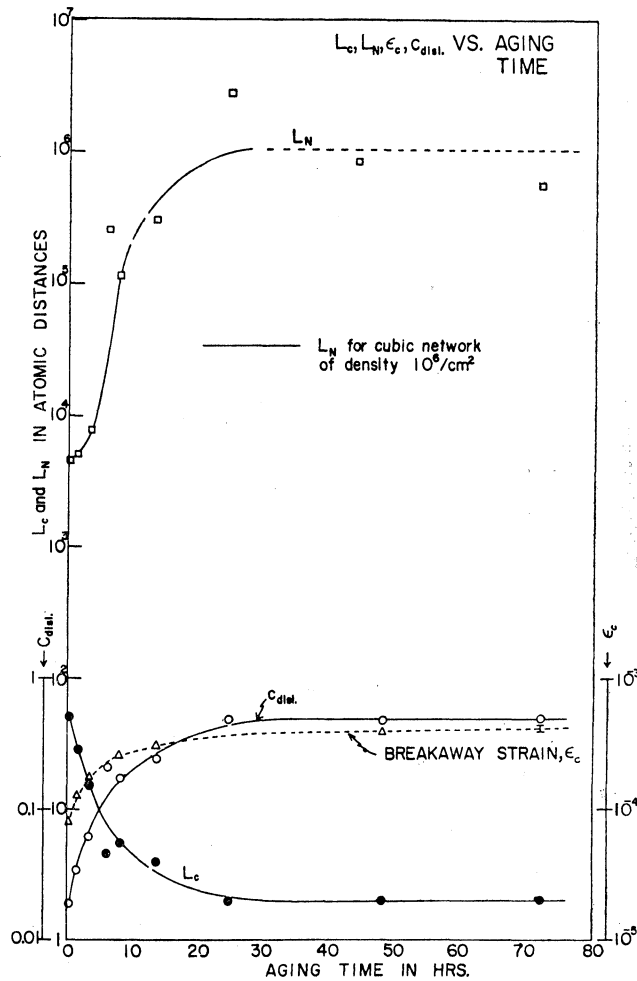


Fig. 8

defects and dislocation by using the following equation,

$$c_{\text{disl.}} = c_0 e^{U/kT}, \quad (7)$$

where c_0 is the bulk concentration, and c_{disl} is the concentration of pinning points on the dislocation, as obtained from L_c . We simply use here the Maxwell-Boltzmann statistics although a refined discussion might be possible with Fermi-Dirac statistics.⁶⁾⁷⁾ Using $c_{\text{disl}}=1/6=0.167$, $c_0=26 \times 10^{-6}$, $kT=1/40$ eV, we obtain 0.22 eV.

If Cottrell's mechanism⁸⁾ of diffusing point defects is here taken into consideration, the number of lattice defects on the dislocation must initially increase as $t^{2/3}$, where t is the elapsed time since the precipitation began. In other words, if we plot the concentration of pinning defects on the dislocation, c_{disl} , against time t in log-log scale, then the points should fall on a straight line with the slope $2/3$. The result is shown in Fig. 9. All points do not fall on a straight line, but over much of the range one can draw a straight line with slope of 0.88, larger than Cottrell's prediction by 31%. This discrepancy will be discussed shortly in connection with the results of time-decay experiments.

Change of breakway stress with time can be easily obtained from Fig. 2. As will be

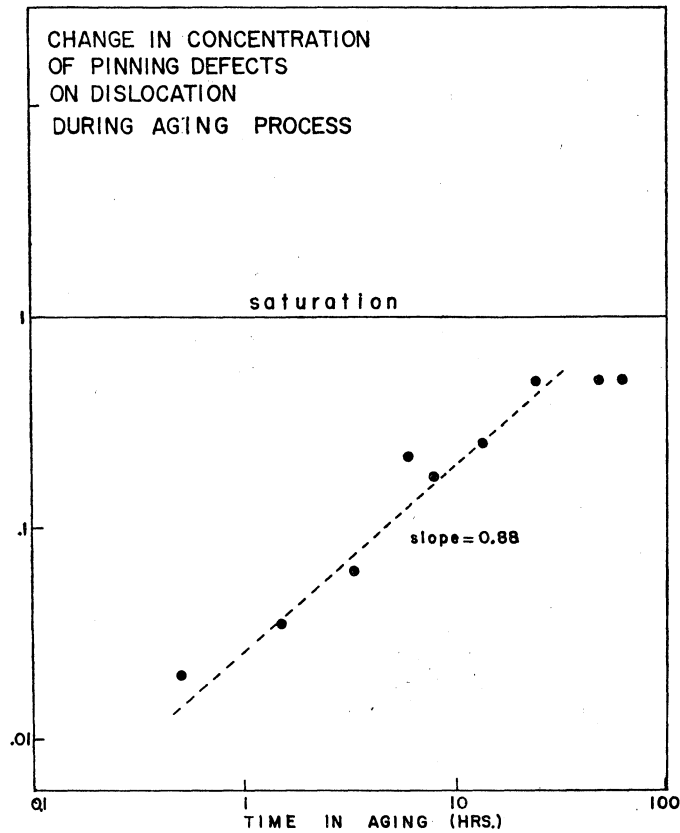


Fig. 10

seen in Fig. 8, the critical stress increases with time and then saturates. Johnston and Gilman⁹⁾ observed in LiF that the stress necessary to move fresh dislocations gradually increases with time after a short annealing at 100°C and finally tends to a saturated value, possibly due to the impurity pinning.

From the formula for δ_H obtained by Granato and Lücke, we get L_N by the following equation:

$$L_N = \sqrt[3]{\frac{\pi K \eta}{\Omega A_0 A} \frac{C_1}{C_2^2}}, \quad (8)$$

where $A_0 = 4(1-\nu)/\pi^2$ in which ν is Poisson's ratio, and C_1 and C_2 are the slope and intersection in the G-L plot with the vertical axis of $\varepsilon^{-1} = 0$. Taking Poisson's ratio ν to be 0.4, A_0 is 0.24. An orientation factor Ω is assumed 1/25 as in G-L paper. Other pertinent numerical values necessary for obtaining L_N are taken as follows:

$$K = 0.31$$

$$\eta = 0.1$$

$$\text{Interatomic distance} = 5 \times 10^{-8} \text{ cm}$$

$$A = 10^6 / \text{cm}^2$$

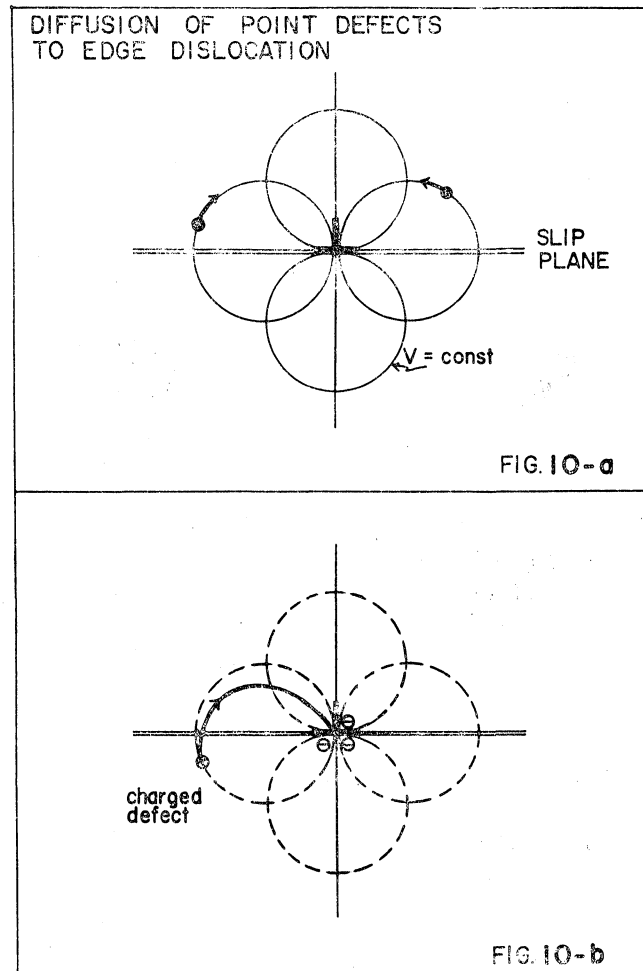


Fig. 10

The dislocation density in AgCl could range from 10^5 to $10^8/\text{cm}^2$. The resulting values for L_N are shown in Fig. 8. L_N is seen initially to increase sharply and then to decrease in the final stage where L_c saturates. However, allowing for the error in determining C_1 , a horizontal line has been drawn. At saturation, $L_N = 10.3 \times 10^5$ atomic distances. Note that L_N increases by a factor of 230 during the entire aging process. This is in contradiction with the basic assumption of G-L theory in which L_N is supposed to be constant. The saturation value of L_N of 10.3×10^5 atomic distances correspond to 516 microns which is approximately ten times larger than that expected on the basis of microscopic observation of dislocation network.¹⁰⁾ Assuming the cubic networks of dislocations with the density $10^6/\text{cm}^2$, the mean internodal distance L_N becomes 15 microns. Even if we assume L_N to be about 10^5 atomic distances, there must still be the change in L_N by a factor of 20. The increase in L_N during aging comes experimentally from the fact that δ_I changes quite slowly in the time sequence while δ_I decreases quite rapidly. In any case, it is no doubt that a considerably large change in L_N takes place during the time sequence.

One possible explanation to this behavior of L_N is as follows: when fresh dislocations

are introduced into a specimen, they may interact with dislocations already present to give the same internodal distance as the aged dislocations. In the course of time, point defects migrate to the dislocation. If some point defects interact with dislocations more strongly than others, but not so strongly as the major pinning points, then for some reason the apparent L_N should increase toward the major pinning distance of aged dislocations. Another explanation of the observed variation of L_N may lie in the fact that the G-L theory only applies at absolute zero temperature; it does not take into account the effect of thermal fluctuations.

The transient change in decrement after mounting, just mentioned, is considered to be identical to the strain ageing phenomena which is caused by the diffusion of divalent impurities. Features which indicate this to be the mechanism of the aging effect of internal friction are as follows: (1) the number of pinning points on the dislocation increases with time and then tends to saturate, thus suggesting the diffusion of point defects to the fresh dislocation; (2) the binding energy calculated from the saturated defect concentration of the same order of magnitude as that obtained by Kabler, Miller, and Slifkin¹⁾ who identified the pinning agents participating in the strain aging in AgCl to be divalent impurities. It has been reported¹¹⁾ that LiF exhibits the same type of transient change in decrement after plastic deformation. Samples doped with divalent impurity show a rapid rate of recovery as compared to purer ones. Sodium chloride also shows time-dependence of decrement after deformation when the sample is kept at high temperature.¹²⁾ The fact that slight handling significantly influences the decrement, as shown in this work, has been also observed in internal friction work on Zn crystal¹³⁾¹⁴⁾¹⁵⁾ and in pure Cu.¹⁶⁾

(b) Analysis of Time Decay of the Strain-Dependent Decrement

In order for time decay of δ_H to take place, the specimen must be "excited", i.e. δ_H must be raised temporarily by means of an externally applied stress, as shown in Fig. 4. The mechanisms involved in the excitation of δ_H are considered to be as follows: (1) the disturbance of charge clouds surrounding dislocation core, as suggested by Remaut, Vennik, Amelinckx¹⁷⁾; (2) the inducing of the breakaway of dislocations from pinning points and, if the situation is favorable, the displacement of the dislocations from one stable position to another; (3) the sliding of pinning points along the dislocations as proposed by Gibbs¹⁸⁾. The last mechanism is dependent on the ease with which the impurity ion can jump under the influence of line tension of dislocations from one site to another along the edge of the extra half plane. Accordingly, the time decay process of δ_H may be caused by building up of charge clouds that had been disrupted by the vibrating dislocation cores, re-accumulation of scattered pinning points, and possible sliding-back of pinning defects to more energetically stable places along the dislocation.

We must consider at this point the nature of charge clouds and pinning defects at dislocations in silver chloride. Experimentally, dislocations in AgCl at temperatures in the extrinsic conductivity region are found to be negatively charged, presumably due to the accumulation of silver vacancies introduced by impurity ion¹⁹⁾²⁰⁾²¹⁾. In order to maintain

charge neutrality, an electrical charge of opposite sign must exist in the region surrounding the dislocation core. This space charge is possibly provided by an excess of positively charged divalent impurity ions. Since the pinning points involved in the strain aging in silver chloride have been demonstrated to be divalent impurity ions, one suspects that impurity ions with an excess positive charge may play roles as both pinning agents and constituents of charge clouds.

If we visualize the pinning of the dislocations by the diffusion of impurity ions to the dislocation, similar to the effect of carbon atoms in the strain aging of α -iron, the number of precipitated impurity ions on the dislocation should be proportional to $2/3$ power of time; that is, one obtains a straight line with the slope of $2/3$ when the logarithm of the concentration is plotted versus the logarithm of the elapsed time. δ_H is related to the concentration in the bulk as

$$\delta_H = Ae^{-Bc}, \quad (9)$$

where A and B are constants independent of the concentration c . If we denote decrement at the beginning of the time decay experiments as $\delta_{H,0}$, then

$$\delta_{H,0} = Ae^{-Bc_0},$$

where c_0 is the defect concentration on the dislocation at the end of excitation. Taking the ratio of δ_H to $\delta_{H,0}$, we get

$$\frac{\delta_H}{\delta_{H,0}} = e^{-B(c-c_0)} = A'e^{-Bc}, \quad (10)$$

where

$$A' = e^{Bc_0}.$$

Assuming the concentration to be proportional to t^n , then

$$\frac{\delta_H}{\delta_{H,0}} = A'e^{-B't^n},$$

where

$$B' \propto B.$$

Using the definition of P as equation (5),

$$P = -B't^n$$

In the $\ln P$ vs. $\ln t$ diagram, the slope is equal to n , if a straight line is obtained. In Fig. 9, where the concentration c obtained from G-L plot has been plotted against the elapsed time, the slope of the best fit line is approximately 0.88. In using the time decay data, shown in Fig. 6, one sees that the slope is in the range between 0.71 to 0.95 with the average close to 0.83. Under the assumptions of the Cottrell mechanism the initial slope is considered to be determined by the velocity of diffusion of the impurities to dislocations. In later stages, the concentration difference between the core and its surrounding will modify the drift velocity. According to Cottrell, the drift velocity v is written as

$$v = - \frac{D}{kT} \nabla V, \quad (11)$$

where D stands for the diffusion coefficient of point defects and V is the elastic interaction given by

$$V = \frac{3}{4} G \eta r_a^3 b \frac{1+\nu}{1-\nu} \frac{\sin \alpha}{r}. \quad (12)$$

The quantities in the equation above are as follows: G is the shear modulus, η is the misfit parameter, r_a is the radius of solvent atom, b is the Burgers vector, ν is Poisson's ratio, and r and α are coordinates relative to the dislocation. Equation (11) shows that a flow of ions is parallel to the gradient of V which has a maximum in a direction perpendicular to the slip plane and a minimum on the slip plane, as shown in Fig. 10-a. Accordingly, the flow of diffusing atoms takes place along the curves drawn perpendicular to the equipotential lines, as indicated arrows in the figure. The direction will depend on the sign of misfit parameter, i.e. for $\eta > 0$, the flow should be toward the expanded region at the bottom of the half-plane and vice versa.

In ionic crystals, the dislocation core bears an electrical charge, with a surrounding charge cloud to maintain electrical neutrality. If we assume that the screening by the charge clouds is not complete for some reason, an electrostatic interaction would be possible between the diffusing defects and the partially unscreened charge on the dislocation. It is interesting to notice in this connection that Sproull²²⁾ measured a microscopic displacement of the order of a few Å of bulk LiF crystal under an applied electric field of high intensity. If the dislocations involved were completely screened by clouds, the displacement of the dislocation core induced by electric field might have been too small to be detected. Also Machlin²³⁾ showed a dependence of the strain-stress relation on the electric field intensity in NaCl, while Neiman and Rothwell²⁴⁾ observed a change in the creep rate in the presence of an electric field in MgO which could be ascribed to the same reason. There is also some evidence that defects produced by gamma irradiation interact electrostatically at liquid nitrogen temperature with dislocations in NaCl²⁵⁾. If the assumption made above is correct, then the diffusing impurity ions see two kinds of interaction forces, elastic and electrostatic. Thus, they migrate to the dislocation along shorter paths than those of Cottrell's theory, which decreases the time required to reach the dislocation core. This means that the rate of decay of decrement may be faster than in the case in which only elastic interaction is important. See Fig. 10-b. It is, however, open to question whether the combination of both interactions gives a linear dependence of the $\ln P$ vs. $\ln t$ diagram.

It is quite interesting that similar time decay experiments on metals, such as Cu¹⁶⁾ and Al²⁶⁾, give a 2/3 power dependence on time. Since the dislocations in metals have no electrical charge, the Cottrell mechanism is considered to represent the situation quite well. Fiore and Bauer²⁷⁾ have shown that in dilute Cu-Ge alloys the binding energy between dislocations and point defects is predominantly elastic, the contribution of

electrostatic and chemical potential being small. This supports the validity of the 2/3 law in metals. It has been known that the recovery of δ_H after mild deformation follows a 2/3 law in NaCl.²⁸⁾ As suggested by Brown and Pratt,²⁹⁾ it seems that diffusing defects involved in strain aging of NaCl are vacancy complexes bearing no net electrical charge, thus explaining 2/3 law.

It is not known at present how much the mechanism of sliding motion of pinning defects on the dislocations may contribute to the time decay of δ_H .

Conclusions

A strong time dependence of decrement has been observed after mounting the specimen in the apparatus at room temperatures. This phenomenon has been identified as a strain aging process; the fresh dislocations introduced by handling are gradually pinned down by the impurity ions with net one electronic charge. The Granato-Lücke analysis shows that the mean distance L_c between minor pinning points decreases with time towards a saturation value of the order of a few atomic distances. The change of breakaway during aging conforms to that of the impurity concentration on dislocations. The saturation value of L_c gives 0.22 eV as the binding energy between impurities and dislocations. The distance L_N between major pinning points appears to increase at least by a factor of 20 during the time sequence of strain aging. This variation may simply reflect inadequacies in the theory. Alternatively, some impurity ions may interact with fresh dislocation comparatively stronger than majority of other minor pins but not so strongly as to act as major pins. This gives an apparently smaller L_N for low stress, but the average L_N should become close to that for aged dislocations for higher stresses. The rate of pinning has been checked by measuring the time decay of δ_H after sufficient excitation. The exponent of t has been determined to be in the range 0.71–1.00 for various runs, a value different from the 0.67 predicted by Cottrell. It is proposed that this higher rate of pinning may be due to the electrostatic interaction between the diffusing point defects and charged dislocations.

Acknowledgements

This research was financially supported in part by the United States Air Force Office of Scientific Research and by the Advanced Research Projects Agency in the United States for an equipment grant.

References

- (1) Kabler, M., Miller, M. and Slifkin, L., *J. Appl. Phys.* **34**, 1953 (1963).
- (2) Blistanov, A., Malakhov, G. and Shaskol'skaya, M., *Soviet Physics-Solid State* **6**, 1934 (1964).
- (3) Shaskol'skaya, M. and Vekilov, Yu., *Soviet Physics-Solid State* **2**, 1001 (1960).
- (4) Fukai, A. and Slifkin, L., *Rep. Fac. Sci. Kagoshima Univ.* **2**, 41 (1969).
- (5) Granato, A. and Lücke, K., *J. Appl. Phys.* **27**, 583 (1956).
- (6) Lothe, J., Technical Report to the Office of Naval Research, Contract No. 760 (08), 1962.
- (7) Louat, N., *Proc. Phys. Soc.* **B69**, 459 (1956).

- (8) Cottrell, A and Bilby, B., Proc. Phys. Soc. **A62**, 49 (1949).
- (9) Johnston, W. and Gilman, J., J. Appl. Phys. **30**, 129 (1959).
- (10) Miller, M., Dissertation, University of North Carolina (1961).
- (11) Blistanov, A. and Shaskol'skaya, M., Soviet Physics-Solid State **6**, 568 (1964).
- (12) Whitworth, R., Phil. Mag. **5**, 425 (1960).
- (13) Read, T., Phys. Rev. **58**, 371 (1940).
- (14) Swift, I. and Richardson, J., J. Appl. Phys. **18**, 417 (1947).
- (15) Wert, C., J. Appl. Phys. **20**, 29 (1949).
- (16) Beshler, D., J. Appl. Phys. **30**, 252 (1959).
- (17) Remaut, G., Vennik, J. and Amelinckx, S., J. Phys. Chem. Solids **16** 158 (1960).
- (18) Gibbs, P., Technical Reprot, No. 3 (July 10, 1957), ONR.
- (19) McGowan, W., Dissertation, University of North Carolina (1965).
- (20) Sonokié, S., Photographic Sensitivity **3**, 1 (1962).
- (21) Sonoiké, S., J. Phys. Soc Japan **17**, 575 (1962).
- (22) Sproull, R., Phil. Mag. **5**, 815 (1960).
- (23) Machlin, E., J. Appl. Phys. **30**, 1109 (1959).
- (24) Neiman, A. and Rothwell, W., Appl. Phys. Lett. **3**, 160 (1963).
- (25) Truell, R., J. Appl. Phys. **32**, 1601 (1961).
- (26) Chambers, R. and Smoluchowski, R., Phys. Rev. **117**, 725 (1960).
- (27) Fiore, N. and Bauer, C., Acta Met. **12**, 1329 (1964).
- (28) Granato, A., Hikata, A. and Lücke, K., Acta Met. **6**, 470 (1958).
- (29) Brown, L. and Pratt, P., Phil. Mag. **9**, 717 (1964).